Differential expression and function of ABCG1 and ABCG4 during development and aging[s]

Dragana D. Bojanic,* Paul T. Tarr,[†] Greg D. Gale,[§] Desmond J. Smith,[§] Dean Bok,**,[††,§§]
Bryan Chen,** Steven Nusinowitz,** Anita Lövgren-Sandblom,*** Ingemar Björkhem,***
and Peter A. Edwards[1],*,[†††,§§§]

Departments of Biological Chemistry* and Medicine,[†††] David Geffen School of Medicine and Molecular
Biology Institute[§§§] at UCLA, Los Angeles, CA 90095; Department of Molecular and Medical Pharmacology,[§]
Jules Stein Eye Institute,** Department of Neurobiology[††] and Brain Research Institute,[§§] Los Angeles, CA
90095; Karolinska Institutet,*** Sweden; and Division of Biology, California Institute of Technology,[†]
Pasadena, CA 91125

Abstract   ABCG1 and ABCG4 are highly homologous members of the ATP binding cassette (ABC) transporter family that regulate cellular cholesterol homeostasis. In adult mice, ABCG1 is known to be expressed in numerous cell types and tissues, whereas ABCG4 expression is limited to the central nervous system (CNS). Here, we show significant differences in expression of these two transporters during development. Examination of β-galactosidase-stained tissue sections from *Abcg1*^{−/−} *LacZ* and *Abcg4*^{−/−} *LacZ* knockin mice shows that ABCG4 is highly but transiently expressed both in hematopoietic cells and in enterocytes during development. In contrast, ABCG1 is expressed in macrophages and in endothelial cells of both embryonic and adult liver. We also show that ABCG1 and ABCG4 are both expressed as early as E12.5 in the embryonic eye and developing CNS. Loss of both ABCG1 and ABCG4 results in accumulation in the retina and/or brain of oxysterols, in altered expression of liver X receptor and sterol-regulatory element binding protein-2 target genes, and in a stress response gene. Finally, behavioral tests show that *Abcg4*^{−/−} mice have a general deficit in associative fear memory.[ɪʟʀ] Together, these data indicate that loss of ABCG1 and/or ABCG4 from the CNS results in changes in metabolic pathways and in behavior.— Bojanic, D. D., P. T. Tarr, G. D. Gale, D. J. Smith, D. Bok, B. Chen, S. Nusinowitz, A. Lövgren-Sandblom, I. Björkhem, and P. A. Edwards. **Differential expression and function of ABCG1 and ABCG4 during development and ageing.** *J. Lipid Res.* 2010. 51: 169–181.

Supplementary key words   oxysterols • liver X receptor • sterol regulatory element binding protein-2 • central nervous system

The mammalian brain represents ~2% of body weight but contains 25% of total body cholesterol, making it the most cholesterol-rich organ in the body (1). Cholesterol homeostasis in the central nervous system (CNS) is unique because, unlike other tissues, it is separated from the general circulation by the blood-brain barrier that prevents the entry of cholesterol-carrying plasma lipoproteins into the CNS (1). Consequently, virtually all the cholesterol in the brain/CNS is thought to result from de novo synthesis (1). The importance of this synthesis can be gauged by the fact that a number of human diseases have been linked to abnormal sterol homeostasis in the CNS; these include cerebrotendinous xanthomatosis and Smith-Lemli-Opitz syndrome (2, 3). Studies with mice defective in sterol homeostasis as a result of inactivation of cholesterol 24-hydroxylase or lathosterol 5-desaturase also identified critical roles for sterols in normal brain function (4, 5).

The retina, although technically part of the CNS, has the capacity both to synthesize cholesterol de novo and to acquire cholesterol from plasma lipoproteins (6). Within the retina, the photoreceptor cells (rods and cones) are the most enriched in cholesterol (7). Indeed, cholesterol is the major sterol of rod outer segment membranes, where it represents 22% of total lipids by weight (8). The importance of maintaining cholesterol concentration in photoreceptors is illustrated by the finding that rhodopsin activation and the visual transduction cascade are impaired when cellular cholesterol levels increase (7). Whether these changes result from an altered membrane environ-

Abbreviations: ABC, ATP binding cassette; CNS, central nervous system; DKO, double knockout; ERG, electroretinography; LTP, long-term potentiation; LXR, liver X receptor; TBST, TBS-1% Tween 20.
[1] To whom correspondence should be addressed.
    e-mail: pedwards@mednet.ucla.edu
[s] The online version of this article (available at http://www.jlr.org) contains supplementary data in the form of one figure.

ment or from a direct interaction of cholesterol with rhodopsin remains to be determined.

ABCG1 and ABCG4 are members of the superfamily of ATP binding cassette (ABC) transporters. This family of proteins utilizes ATP hydrolysis to transport a wide variety of substrates across various cellular membranes (9). ABCG1 and ABCG4 are closely related half-transporters that share 69% identity (82% similarity) at the amino acid level. When overexpressed in vitro, these two proteins can form either homo- or heterodimers (10). Both mammalian proteins have high amino acid similarity (~43%) to the *Drosophila* white gene, the founding member of this family of transporters. The *Drosophila* white gene forms obligate heterodimers with two other ABC transporters (scarlet or brown) and plays an essential role in eye pigmentation (11). However, recent studies have shown that neither ABCG1 nor ABCG4 can functionally replace the white gene since eye pigmentation was still defective in *white*$^{-/-}$ flies that overexpress either ABCG1 or ABCG4 (12).

Mammalian ABCG1 is expressed in many cell types (including macrophages, endothelial and epithelial cells, T and B cells, type II cells, astrocytes, and neurons) and in numerous tissues, including the brain, eye, kidney, spleen, lung, liver, and intestine (13–15). In contrast, several studies have demonstrated that ABCG4 expression is highly restricted to the eye and to astrocytes and neurons of the brain/CNS (15–18). One other important difference between the two genes is their response to the nuclear receptor liver X receptor (LXR); activation of LXR induces the expression of *Abcg1* mRNA and protein but has no effect on the expression of *Abcg4* (18).

Studies utilizing *Abcg1*$^{-/-}$ LacZ knockin mice established a critical role for ABCG1 in cellular cholesterol homeostasis in the lung; loss of ABCG1 resulted in massive accumulation of macrophage foam cells that were loaded with sterols and significant increases in pulmonary surfactant (13, 19, 20). In addition, studies employing either macrophages derived from *Abcg1*$^{-/-}$ mice or cells that overexpress ABCG1 have shown that ABCG1 effluxes cellular cholesterol to a variety of exogenous acceptors, including HDL, LDL, liposomes, and cyclodextrin (13, 14, 21). Not surprisingly, overexpression of the highly homologous ABCG4 protein in cultured cells also stimulates sterol efflux to exogenous HDL (22–24).

Unlike ABCG1, ABCG4 is not expressed in tissues and cells outside the CNS in adult mice. Insights into the potential importance of ABCG4 and ABCG1 in the CNS have come from studies with *Abcg1*$^{-/-}$ *Abcg4*$^{-/-}$ double knockout (DKO) and single knockout mice; the brains of DKO mice contained increased levels of 27-hydroxycholesterol and a number of cholesterol precursors, including desmosterol, lathosterol, and lanosterol (15). The changes in sterol composition in the DKO mice were more severe than in the single knockout mice, consistent with a role for both ABCG1 and ABCG4 in sterol homeostasis in the brain (15). More recently, it was suggested that ABCG4 may play a role in the development of Alzheimer's disease since ABCG4 levels were reported to be increased in the brains of patients with Alzheimer's disease (25). Whether this represents a direct or indirect link will require additional studies.

In this study, we used several techniques to investigate the expression and function of ABCG1 and ABCG4 during development. Analysis of both *Abcg1*$^{-/-}$ *LacZ* and *Abcg4*$^{-/-}$ *LacZ* knockin embryos identified, for the first time, cells that express ABCG4 in the absence of detectable ABCG1. We also show that both ABCG1 and ABCG4 are highly expressed in neurons of the adult retina and that expression is detectable in these cells as early as E15.5. Targeted disruption of *Abcg1* and/or *Abcg4* led to the accumulation of various sterol intermediates and oxysterols and to changes in the expression of LXR target genes and genes involved in cholesterol and fatty acid biosynthesis, cholesterol oxidation, and stress in both the retina and brains of these mice. Despite these changes in the retina, electroretinograms were normal. However, we report here that loss of ABCG4 is associated with changes in contextual fear.

EXPERIMENTAL PROCEDURES

Animals

Abcg1$^{+/-}$ *LacZ* and *Abcg4*$^{+/-}$ *LacZ* mice were obtained from Deltagen as previously described (13, 18). Mice heterozygous for gene deletion were backcrossed multiple times to C57BL/6 mice (13, 18) and then intercrossed to generate homozygous single knockout mice. Subsequently, *Abcg1*$^{-/-}$ *Abcg4*$^{-/-}$ double knockout mice were generated by intercrossing *Abcg1*$^{-/-}$ and *Abcg4*$^{-/-}$ single knockout mice.

β-Galactosidase staining of embryos and tissue sections

Mouse embryos of gestational age 10.5, 12.5, and 15.5 days were dissected in PBS and fixed for 4 h at 4°C in 4% paraformaldehyde/0.1 M phosphate buffer (pH 7.4). The embryos were rinsed three times in PBS and incubated for 16 h at room temperature in the dark in 100 mM phosphate buffer, 2 mM MgCl$_2$, 5 mM K$_3$Fe(CN)$_6$, 0.02% (v/v) Nonidet P-40, and 1 mg/ml X-gal (5-bromo-4-chloro-3-indolyl-β-D-galactopyranoside). Following staining, embryos were washed three times for 15 min each with PBS/0.1% Tween 20 and transferred to 4% paraformaldehyde/0.1 M phosphate buffer (pH 7.4) and then photographed using a Leica DC500 digital camera. For cell type-specific staining, fixed embryos were cryoprotected, sectioned, and stained for β-galactosidase activity as previously described (13). Briefly, embryos were fixed and washed, as described above, before being cryoprotected by incubation in 20% sucrose in PBS at 4°C overnight. Embryos were snap-frozen in OCT and stored at −80°C until sectioned. Ten micrometer sections were transferred to glass slides and stained for β-galactosidase activity as described above for whole embryos. After overnight staining and washing, slides were counterstained with nuclear fast red, rinsed with water, dehydrated, and mounted under coverslips using a xylene-based mounting medium.

In situ hybridization

Two 8 month old mice (C57BL/6) were enucleated, lenses were removed, and eyecups were incubated in 4% paraformaldehyde/0.1 M phosphate buffer (pH 7.4) for 3.5 h at 4°C with constant rotation. Fixed retinas were cryoprotected by emersion in 20% sucrose in PBS at 4°C for 1 h and snap-frozen in OCT. Frozen sections (10 µm) were allowed to adhere to glass slides, air dried for 1 h, and stored at −80°C until used. Sections

were bleached in 0.5% H_2O_2, permeabilized with proteinase K (1 µg/ml), treated with prehybridization buffer (50% formamide, 5× SSC at pH 4.5, 1% SDS, 50 µg/ml torula RNA, and 50 µg/ml heparin) for 30 min at 70°C, and hybridized with either *Abcg1* or *Abcg4* sense or antisense digoxigenin-labeled cRNA probes (1 µg/ml) overnight at 70°C. Sections were washed three times for 15 min each in Solution 1 (50% formamide, 5× SSC, pH 4.5, and 1% SDS) at 70°C, three times for 15 min each in Solution 2 (50% formamide and 2× SSC, pH 4.5) at 65°C, and three times for 10 min in TBS-1% Tween 20 (TBST) at room temperature. After blocking in 5% sheep serum/TBST for 1 h at room temperature, the sections were incubated with alkaline phosphatase-conjugated sheep anti-digoxigenin antibody (1:2,000) in 1% sheep serum/TBST at room temperature for 2 h. The alkaline phosphatase reaction was performed in the presence of nitro blue tetrazolium in order to visualize the mRNA. The reaction was stopped with acidic PBS containing 1% Tween 20.

RNA isolation and analysis

Total RNA was isolated from retinas and half brains from 2 or 7 month old mice using Trizol reagent (Invitrogen), and 1 µg of total RNA was treated with DNase and then reverse transcribed with random hexamers using SuperScript II (Invitrogen). Quantitative real-time PCRs were performed using the IQ Sybr Green Supermix (Bio-Rad) using the MyIQ real-time PCR detection system (Bio-Rad). Results of quantitative PCR were evaluated by the comparative cycle number determined at threshold method and normalized to GAPDH or β-actin. Primer sequences are available upon request.

Sterol analysis in brain and retina

Levels of cholesterol, lathosterol, and oxysterols in the brain and retina of 8 month old mice were determined by isotope dilution-mass spectrometry as previously described using known standards (26–28).

Electron microscopy

Tissues for electron microscopy were processed as described (29).

Electroretinography

Six month old mice, overnight dark-adapted, were anesthetized with an intraperitoneal injection of normal saline containing ketamine (15 mg/g body weight) and xylazine (3 mg/g body weight). Electroretinographs (ERGs) were recorded from the corneal surface of one eye after pupil dilation (1%, w/v, atropine sulfate in saline buffer) using a gold-loop electrode referenced to a similar gold wire in the mouth as described (30). Briefly, all stimuli were generated with a photic stimulator (model PS33 Plus; Grass-Telefactor) affixed to the outside of the dome at 90° to the viewing porthole. ERGs were recorded to a series of blue (Wratten 47 A; λmax = 470 nm) flashes of increasing intensity, ranging from –4.7 to –0.44 log cd-s/m². Responses were sampled at 1 kHz, amplified (CP511 AC amplifier, ×10,000; Grass-Telefactor), and digitized using an I/O board (PCI-1200; National Instruments) in a personal computer. Signal processing was performed with custom-written software. For each stimulus, responses were computer averaged with up to 50 records averaged for the weakest signals. A signal rejection window could be adjusted online to eliminate artifacts.

Fear conditioning

Learning and memory were assessed through a Pavlovian fear conditioning procedure using 7 month old mice as described (31, 32). Initial training was conducted in a modified Gemini Avoidance System (San Diego Instruments). The chamber had white plexiglass walls and a clear plexiglass ceiling (H, 25 cm; W, 22 cm; D, 18 cm). The floor of the chamber consisted of 12 stainless steel rods (2 mm diameter, 1.2 cm apart) connected to the shock generator. Tones were presented from a speaker mounted in one wall of the chamber. Indirect lighting (∼200 Lux) was provided by a floodlight placed next to the apparatus. Mice were given a 3 min habituation period prior to a delay fear conditioning procedure consisting of 3 tone (2 kHz, 80 db, 15 s)/footshock (0.6 mA, 1 s) pairings delivered at 1 min intervals. Mice were removed from the chamber 2 min after the final pairing.

Context fear testing

One day after conditioning, mice began a contextual fear extinction series. On four consecutive days, at 24 h intervals, mice were returned to the conditioning chamber for a 6 min extinction test.

Cued fear testing

One day after the final contextual extinction session, mice were assessed for context generalization and cued fear. Testing was conducted in a novel rectangular chamber (L, 50 cm; W, 25 cm; H, 25 cm) with white laminated flooring and white plexiglass walls. After a 3 min baseline period, 6 CS (2 kHz, 80 db, 20 s), presentations were delivered with a 1 min ITI. Mice were removed from the chamber 2 min after the final cue presentation.

Behavioral analysis

For all test sessions, behavior was recorded from video cameras mounted above the apparatus then digitized at 15 frames per second with the EthoVision Pro tracking system (Noldus Information Technology). For each test, we quantified a range of behavioral endpoints, including velocity, path shape variables (turn angle and meander), place preference measures (thigmotaxis, corner preference), and immobility. All endpoints were estimated continuously by comparing pairs of consecutive samples. Velocity was defined as the distance moved by the animal's center of gravity per unit time. Turn angle was defined as the average change in heading, in degrees, across two consecutive samples, where heading equaled the direction of movement relative to a reference line established over the preceding two samples. Meander was defined as the average turn angle per distance moved. Thigmotaxis for all tests was calculated as the percentage of time spent in the periphery of the apparatus, defined as the area within 5 cm of the wall.

Statistical analysis

Behavioral tests were performed on wild-type (n = 10), $Abcg1^{-/-}$ (n = 7), $Abcg4^{-/-}$ (n = 6), and $Abcg1^{-/-}Abcg4^{-/-}$ (n = 14) mice. All mice were 7 months old. To assess potential group differences, we performed one-way ANOVA on each individual endpoint. Fear conditioning endpoints were calculated independently for the preshock and postshock periods. Contextual fear endpoints were calculated for each 6 min test session. Contextual extinction rates were estimated through repeated-measure ANOVA on time course data (5 s bins). Cued fear endpoints were calculated independently for the 3 min baseline period and the CS presentation period. Significant group differences were characterized with posthoc analysis using Tukey-Kramer honestly significant difference test. A significance threshold of $P < 0.05$ was used for all tests.

Morris water maze

Morris water maze tests were performed on 14 wild-type and 14 $Abcg1^{-/-}Abcg4^{-/-}$ mice (7 months old) as described (33).

Differential expression of ABCG1 and ABCG4 during development

We previously characterized adult mice in which either the *Abcg1* or *Abcg4* gene was disrupted as a result of the insertion of the bacterial *LacZ* gene into exon 3 or exon 14, respectively (18). In these knockout/knockin mice, the promoters of the endogenous *Abcg1* or *Abcg4* genes control the expression of β-galactosidase (18). Importantly, the β-galactosidase protein is targeted to the nuclei as a result of the insertion of a nuclear localization signal (18). Thus, β-galactosidase-positive nuclei serve as a marker for the normal cellular expression and regulation of the corresponding endogenous ABCG gene.

To elucidate the expression pattern of ABCG1 and ABCG4 during fetal development, whole mouse embryos were obtained from pregnant *Abcg1*$^{-/-}$ *LacZ* or *Abcg4*$^{-/-}$ *LacZ* knockin mice, (abbreviated to *Abcg1*$^{-/-}$ or *Abcg4*$^{-/-}$) at different stages of embryonic development and stained for β-galactosidase activity (**Fig. 1A**). Analysis of the stained embryos indicated that ABCG4 is expressed in the fetal liver at E10.5, E12.5, and E15.5 (Fig. 1A, panels a–c). Although β-galactosidase was undetectable in other embryonic tissues of the *Abcg4*$^{-/-}$ embryos at E10.5, we observed high expression in the developing eye and CNS at both E12.5 and E15.5 (Fig. 1A, panels b and c).

To better characterize the LacZ-expressing cells in the whole mounts of Fig.1A, we also stained tissue sections obtained from E15.5 embryos, new born pups (P0), and adult mice for β-galactosidase activity. The data indicate that ABCG4 is highly expressed in hematopoietic cells that populate the fetal liver at E15.5, but hepatic expression is barely detectable at P0 and absent from the livers of adult mice (Fig. 1B, panels a–c). Surprisingly, we also noted that ABCG4 is highly expressed in enterocytes that line the ileum at P0 (**Fig. 2a**). This expression of ABCG4 in enterocytes is transient since activity is undetectable in intestinal sections taken from *Abcg4*$^{-/-}$ adult mice (Fig. 2b).

The data of Figs. 1 and 2 identify significant differences in expression of β-galactosidase in *Abcg4*$^{-/-}$ and *Abcg1*$^{-/-}$ mice during development. For example, at E10.5, β-galactosidase expression was restricted to the olfactory pit in the *Abcg1*$^{-/-}$ embryo (Fig.1A, panel d), with no discernable staining of the fetal liver. However, by E12.5 multiple tissues, including the CNS and eye stained intensely for β-galactosidase activity (Fig. 1A, panel e), although expression in the liver remained very low (Fig. 1A, panel e, white arrow). By E15.5, staining of the *Abcg1*$^{-/-}$ embryos was so intense and ubiquitous that only the eye and whiskers could be clearly discerned (Fig. 1A, panel f). We note that the expression of ABCG1 in the CNS and retina during development parallels that reported by Annicotte, Schoonjans, and Auwerx (34) for LXRβ, a nuclear receptor known to activate *Abcg1*.

Analysis of stained tissue sections confirmed the differences in expression of ABCG1 and ABCG4. For example, hepatic ABCG1 expression is limited to Kupffer cells and endothelial cells, a pattern of expression that persists from E15.5 through adulthood (Fig. 1B, panels d–f). We also
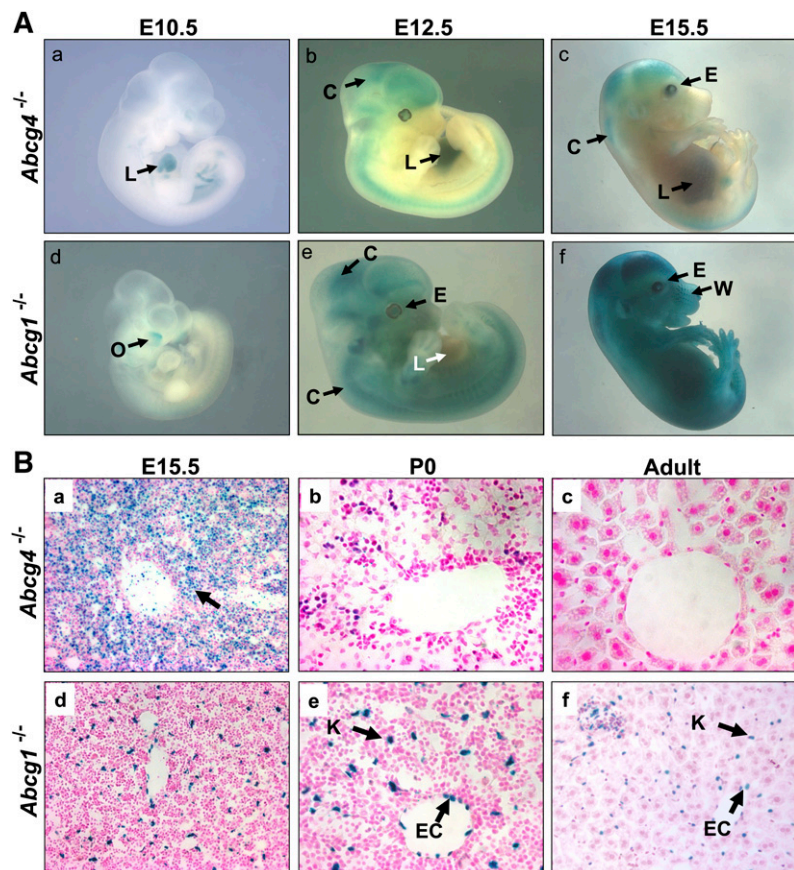

Fig. 1. Differential expression of ABCG1 and ABCG4 during mouse embryonic development. A: Whole mouse embryos with the indicated genotype were isolated at E10.5 (a and d), E12.5 (b and e), and E15.5 (c and f) and stained for β-galactosidase activity (blue-stained cells/tissues). The olfactory pit (O), liver (L), eye (E), whiskers (W), and CNS (C) are indicated. The white arrow indicates the relatively poorly stained liver of the *Abcg1*$^{-/-}$ embryo. B: Tissue sections from livers of the indicated mouse genotypes were stained for β-galactosidase activity. ABCG4 is highly expressed in fetal hematopoietic cells at E15.5 (a), barely detectable at P0 (b), and absent from adult liver (c). ABCG1 is highly expressed in Kupffer cells (K) and endothelial cells (EC) of the mouse liver between E15.5 and adulthood (d–f).
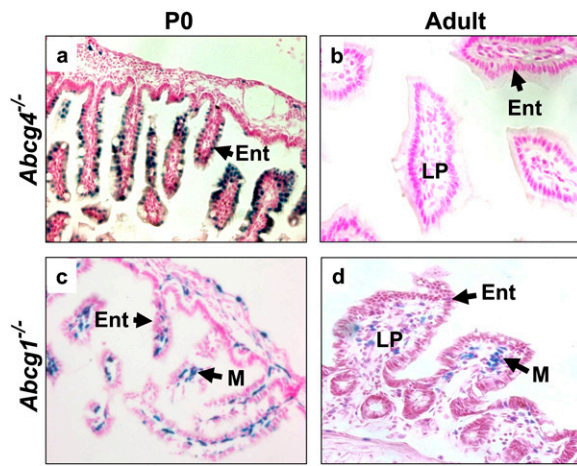
Fig. 2. High expression of ABCG4, but not ABCG1, in enterocytes of the developing intestine. Tissue sections of the intestine were stained for β-galactosidase activity. ABCG4 is transiently expressed in enterocytes at P0 (a) but absent from the intestine in the adult mouse (b). ABCG1 is highly expressed in the macrophages (M) of the lamina propria (LP) but absent from enterocytes (Ent) lining the intestine of P0 (c) and adult mice (d).

Fig. 3. ABCG1 and ABCG4 are coexpressed in the CNS at E15.5. β-Galactosidase-stained sections of the CNS identify ABCG1 and ABCG4 expressing neurons as early as E15.5. Both ABCG4 and ABCG1 are expressed in the choroid plexus (CP) (a and c), dorsal root ganglion (DRG) (b and d), and the motor neurons (MN) in the spinal cord (b and d). The inset in panel a shows a higher magnification of the choroid plexus from a different section of the $Abcg4^{-/-}$ brain.

show that ABCG1 expression in the intestine is limited to macrophages present in the lamina propria of both new born pups (P0) and adult mice and is absent from the enterocytes at all stages of development (Fig. 2c, d). Together, these studies identify, for the first time, cells (enterocytes and fetal hematopoietic cells) that express high levels of ABCG4 but little or no ABCG1. However, to date, no phenotype has been identified that is associated with the loss of ABCG4 from these cells.

We and others have previously utilized LacZ knockin mice to demonstrate that ABCG1 and ABCG4 are coexpressed in neurons of the CNS of adult mice (15, 18). Based on β-galactosidase-stained tissue sections, we had also noted that ABCG1, but not ABCG4, was highly expressed in the epithelial cells that form the choroid plexus and endothelial cells that line the blood vessels of the adult mouse brain (18). Unexpectedly, the current studies show that both ABCG4 and ABCG1 are expressed in the epithelial cells of the choroid plexus at E15.5 (**Fig. 3a**, c). However, the expression of β-galactosidase/ABCG4 observed in the choroid plexus of E15.5 embryos was transient, as it was undetectable in the corresponding tissue of adult knockin mice (data not shown) (18). Consistent with the intense staining of the CNS in developing wholemount embryos (Fig. 1A), we show that neurons present in the dorsal root ganglion and spinal cord of both $Abcg1^{-/-}$ and $Abcg4^{-/-}$ mice stain positively for β-galactosidase activity at E15.5 (Fig. 3b, d). The effects of loss of ABCG1 and/or ABCG4 on neuronal function are discussed below.

Expression of ABCG1 and ABCG4 in the mouse retina

The data of Fig. 1A demonstrate that both ABCG1 and ABCG4 are highly expressed in the eyes of the developing embryos as early as E12.5. Analysis of sections taken from
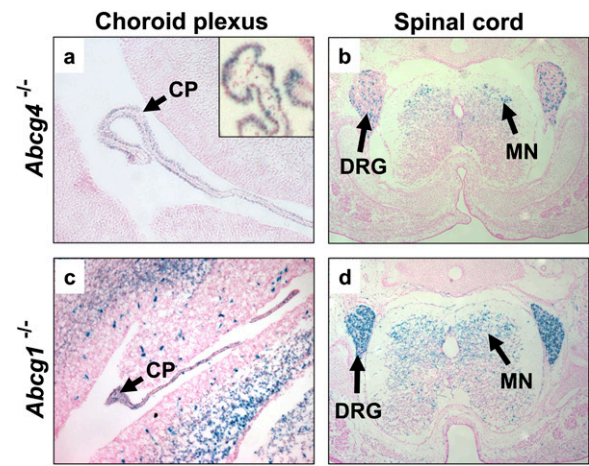
the eye (**Fig. 4A**, panel a) or retinas (Fig. 4A, panels b and d) shows that in early stages of embryonic development (E15.5), ABCG4 and ABCG1 are more highly expressed in the ganglion cells. However, in adult mice, the neurons present in the outer and inner nuclear layer of the retinas are particularly intensely stained (Fig. 4A, panels c and e). Indeed, we have noted that of all the tissues examined in the adult $Abcg1^{-/-}$ or $Abcg4^{-/-}$ knockout mice, β-galactosidase is most highly expressed in the neurons present in the retina (Fig. 4) and in the CA regions of the hippocampus (18).

We predicted that loss of functional ABCG1 or ABCG4 would disturb cellular sterol homeostasis and result in activation of LXR and its target genes (see below). Since β-galactosidase expression in the $Abcg1^{-/-}$ mouse is under the control of the endogenous regulatory elements (including multiple LXREs) that normally control transcription of the $Abcg1$ gene, we hypothesized that activation of LXR in these knockout mice would increase β-galactosidase expression and activity. Consequently, we also stained tissue sections from the retinas of heterozygous mice. As expected, the staining pattern for β-galactosidase activity in the retinas of heterozygous and knockout $Abcg1$ or $Abcg4$ mice was indistinguishable (data not shown). Nonetheless, we also performed in situ hybridization using retinas derived from adult wild-type mice where LXR activation would not be affected by loss of an ABC transporter; the data show clearly that both $Abcg1$ and $Abcg4$ mRNAs are highly expressed and localized to the neuronal cells of the adult retina of C57BL/6 mice (Fig. 4B, panels a and b). Little or no staining was observed with sense probes (Fig. 4B, panels c and d). Thus, studies with both wild-type, heterozygote, and knockout mice indicate that both ABCG1 and ABCG4 are highly expressed in neurons in the retina.
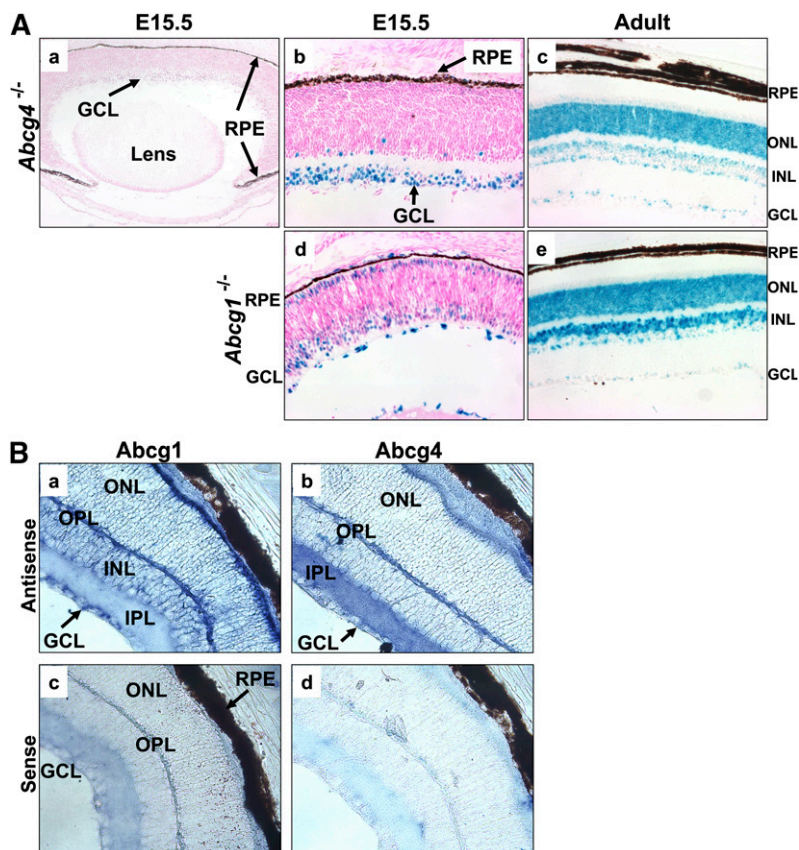
Fig. 4. ABCG1 and ABCG4 are highly expressed in the mouse neural retina. A: Sections of the mouse eye or retina were stained for β-galactosidase activity. The blue stain identifies both ABCG1 and ABCG4-expressing cells in the ganglion cell layer (GCL) at E15.5 (a, b, and d). Intense staining was detected in the photoreceptor cell bodies of the outer nuclear layer (ONL), neuronal cell bodies of the inner nuclear layer (INL) in the adult mouse (c and e). RPE, retinal pigment epithelium is unstained. B: In situ hybridization identified cells coexpressing high levels of *Abcg1* and *Abcg4* mRNAs in the 8 month old C57BL/6 mouse retina. Sections of the retina obtained from wild-type C57BL/6 mice were hybridized with digoxigenin-labeled antisense probes to *Abcg1* (a) or *Abcg4* (b) or sense probes to *Abcg1* (c) or *Abcg4* (d) as described in Experimental Procedures. *Abcg1* and *Abcg4* mRNA are visualized as a blue reaction product. IPL, inner plexiform layer.

Effect of loss of ABCG1 and/or ABCG4 on the mouse retina

Loss of function of the ABC transporter ABCA4 (ABCR) from mice or humans is associated with various retinal defects (35). In mice, the observed defects depend on the genetic strain of mice; $Abca4^{-/-}$ mice on albino background, but not on a C57BL/6 background, show changes in organization of the rods and cones as determined by electron microscopy and changes in the response of the retinal cells to light as determined by electroretinography (36, 37). Based on the latter studies, we determined whether loss of ABCG1 and/or ABCG4 affects retinal function. In attempts to identify altered function, we performed ERG under both dark- and light-adapted conditions, in order to distinguish between potential effects on rods versus cones, respectively. However, there was no significant difference between wild-type, $Abcg1^{-/-}$, $Abcg4^{-/-}$, or $Abcg1^{-/-}Abcg4^{-/-}$ mice (**Fig. 5A**, B). Consequently, we conclude that the response of rods or cones to light are unaffected by loss of these two cholesterol transporters. In addition, detailed analyses of multiple electron micrographs obtained from both wild-type and $Abcg1^{-/-}$ retinas failed to identify any significant differences (Fig. 5C).

We also considered that loss of ABCG4 and/or ABCG1 might affect sterol homeostasis and gene expression in the retina. To test this proposal, we profiled retinal mRNAs obtained from wild-type and $Abcg1^{-/-}Abcg4^{-/-}$ (DKO) mice using a PCR-based Mouse Signal Transduction Pathway-Finder (SuperArray). This approach identified a number of genes that were differentially expressed (data not shown). We then used quantitative RT-PCR to confirm these predictions. As shown in **Fig. 6**, a number of mRNAs that include the *Lxr* target genes *Abca1* and *Abcg1* are induced in retinas obtained from 2 month old DKO mice. In these knockout mice, *Abcg1* mRNA levels were determined using primers that amplify exon1 to exon 2. Importantly, since $Abcg1^{-/-}$ mice were generated by knocking in *LacZ* into exon 3, both exon 1 and 2 are normally expressed from the endogenous promoter in both wild-type and $Abcg1^{-/-}$ mice.

In addition to altered expression of two *Lxr* target genes, the data in Fig. 6 show that loss of both ABCG1 and ABCG4 resulted in increased expression of *Egr-1*, a gene that is induced in response to various cellular stresses. Surprisingly, there was no significant difference in the level of the LDL receptor (*Ldlr*) mRNA or other genes involved in cholesterol homeostasis in the retinas of wild-type and DKO mice (Fig. 6) (data not shown). Nonetheless, taken together, these data indicate that loss of both ABCG1 and ABCG4 from the mouse retina results in activation of LXR and changes in gene expression associated with cellular stress. These data also suggest that sterol composition might be altered in the retinas of DKO mice. Consistent with this proposal, we show that lathosterol levels are significantly increased in retinas obtained from DKO mice (**Table 1**). However, the concentrations of a number of oxysterols, some of which are known to activate LXR, were not significantly different in retinas from the two genotypes (Table 1).
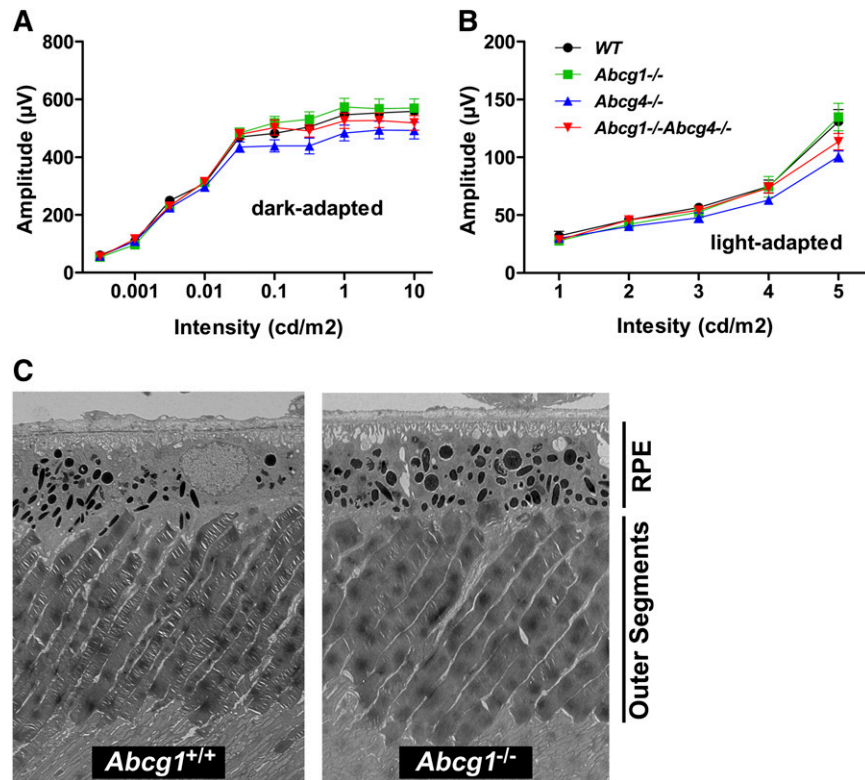
Fig. 5. Targeted disruption of *Abcg1*, *Abcg4* or both genes in mice has no effect on retinal function and structure. ERG responses were recorded from *Abcg1*$^{-/-}$ (squares), *Abcg4*$^{-/-}$ (upwards triangles), *Abcg1*$^{-/-}$ *Abcg4*$^{-/-}$ (downwards triangles), and wild-type (circles) mice at 6 months of age (n = 5 per group) under dark adaptation conditions (A) and under light adaptation conditions (B) as described in Experimental Procedures. C: Representative electron micrographs of the retinas from 8 month old wild-type and *Abcg1*$^{-/-}$ mice reveal no significant structural difference. RPE, retinal pigment epithelium.

Effect of loss of ABCG1 and/or ABCG4 on gene expression in the brain

A recent report has shown that the brains of *Abcg1*$^{-/-}$ *Abcg4*$^{-/-}$ mice contained increased levels of 27-hydroxycholesterol and certain precursors of cholesterol (15). These latter data, together with the current studies
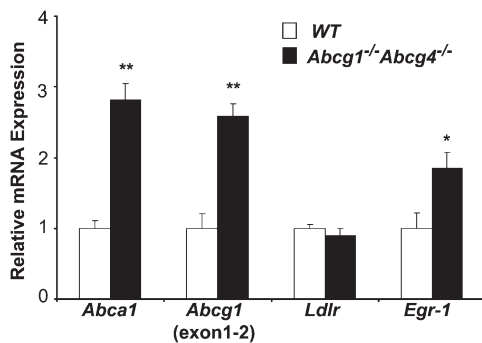

Fig. 6. Altered expression of genes involved in cholesterol homeostasis and stress response in the retinas of *Abcg1*$^{-/-}$ *Abcg4*$^{-/-}$ mice. mRNA expression levels of *Abca1*, *Abcg1* (*exon 1-2*), *Ldlr*, and *Egr-1* were quantified in the retinas of 2 month old wild-type (n = 4) and *Abcg1*$^{-/-}$ *Abcg4*$^{-/-}$ DKO (n = 5) mice using quantitative RT-PCR. Ldlr, low density lipoprotein receptor; *Egr-1*, early growth response gene 1. All samples were normalized to *Gapdh* (glyceraldehyde 3-phosphate dehydrogenase). Values are given as means ± SEM. * $P < 0.05$; **$P < 0.005$.

on the retinas from DKO mice (Figs. 4 and 6) suggest that deletion of ABCG1 and ABCG4 would result in changes in gene expression in the brain. To test this proposal and to assess whether the changes were age dependent, we quantified specific mRNAs in the brains of 2 and 7 month old DKO and wild-type mice.

The data show that mRNA levels of HMG-CoA reductase (*Hmgr*), farnesyl diphosphate synthase (*Fpps*), and *Ldlr* are repressed in the DKO brains in an age-dependent manner; mRNA levels were not significantly different at 2 months of age but were decreased significantly by 7 months (**Fig. 7A**). The mRNAs encoding lanosterol demethylase (*Cyp51*) and cholesterol 27-hydroxylase (*Cyp27a1*) were also repressed in the brains of the older DKO mice (Fig. 7A). The importance of the observed changes in *Cyp27a1* mRNA levels is unclear, as we noted that the levels of this mRNA are extremely low in the brains of both genotypes. Importantly, not all *Cyp* genes were repressed as mRNA levels of *Cyp46a1*, encoding cholesterol 24-hydroxylase, were increased in the brains of the older DKO mice (Fig. 7A). These changes in gene expression suggest that sterol homeostasis was altered in the CNS following loss of ABCG1 and ABCG4.

The most striking changes in gene expression in the DKO brains involved specific LXR target genes; *Abcg1* (as determined by quantification of exon1-2) and *Abca1* were highly induced in both 2 and 7 month old DKO brains

Sterol	Wild Type (n = 14)	$Abcg1^{-/-} Abcg4^{-/-}$ (n = 14)
Cholesterol	4.45 ± 0.3	5.18 ± 0.3
24(S)-OH-cholesterol	1.04 ± 0.1	1.24 ± 0.09
25-OH-cholesterol	ND	ND
27-OH-cholesterol	0.05 ± 0	0.06 ± 0
Lathosterol	155.1 ± 10	209.6 ± 13*

Retinas (total 56) were obtained from 14 wild-type and 14 DKO 8 month old mice. Seven retinas with the same genotype were combined to generate four wild-type and four DKO samples (n = 4 samples per genotype). Sterols were extracted and analyzed as described (26–28) using isotope dilution-mass spectrometry. Data are presented as μg (cholesterol) or ng (other sterols) per mg of protein. Values shown are mean ± SEM. $P < 0.05$. ND, not detectable.

(Fig. 7B). A third LXR target gene, *Srebp-1c*, was induced at 2 months, but there was no significant change in the brains of the older DKO mice (Fig. 7B). Based on analysis of the brain and retina, we conclude that transcription of both *Abcg1* and *Abca1* genes is more sensitive to activation by

Fig. 7. Age-dependent expression of genes involved in lipid homeostasis in the brains of $Abcg1^{-/-} Abcg4^{-/-}$ mice. mRNA levels of genes involved in cholesterol metabolism were determined by quantitative RT-PCR analysis of RNA extracted from whole brains from 2 month old wild-type (n = 5) and $Abcg 1^{-/-} Abc^{-/-}$ DKO (n = 5) mice and 7 month old wild-type (n = 9) and $Abcg1^{-/-} Abcg4^{-/-}$ DKO (n = 9) mice. A: *Hmgr*, HMG-CoA reductase; *Fpps*, farnesyl diphosphate synthase; *Ldlr*, low density lipoprotein receptor; *Cyp51*, lanosterol 14α-demethylase; *Cyp27a1*, sterol 27-hydroxylase; *Cyp46a1*, cholesterol 24-hydroxylase. B: *Srebp-1c*, sterol regulatory element binding protein 1c; *Scd-1*, stearoyl-CoA desaturase-1, *Egr-1*, early growth response gene 1. mRNA levels were normalized to β-actin. Values are given as mean ± SEM. * $P < 0.05$; ** $P < 0.005$.

LXR than *Srebp-1c*. Interestingly, the mRNA levels of steroyl CoA desaturase 1 (*Scd-1*), a gene that is known to be activated by both SREBP-1c and LXR (38), was also induced in the brains of 2 but not 7 month old DKO mice, thus paralleling the changes in expression of *Srebp-1c* (Fig. 7B).

Finally, we show that the stress-induced gene *Egr-1* that is induced in the retinas of DKO mice (Fig. 6) is also induced in the brains of the 2 month, but not 7 month, old DKO mice, thus paralleling the changes in *Scd*-1 and *Srebp-1c* in the brain (Fig. 7B). In contrast, mRNAs corresponding to other stress-induced genes that include the heat shock response gene *Hsf-1* and genes involved in the unfolded protein response (*Perk*, *Ire1*, *Chop*, *Bip*, and *Atf6*) were expressed at similar levels in the brains of 2 or 7 month old wild-type and DKO mice (data not shown). Additional quantitative RT-PCR analyses demonstrated that the brain expression of two well-characterized RAR/RXR target genes (*Hnf-3α* and *Rbp-1*) was unaffected following loss of both ABCG1 and ABCG4 (data not shown). These latter data suggest that RAR/RXR activation by retinoids is not affected in the DKO mice. Taken together with the analysis of the retinas from DKO mice, we conclude that loss of both ABC transporters results in an age-dependent activation of LXR and specific LXR target genes, to changes in expression of genes regulating lipid synthesis and to increased cellular stress. We hypothesize that compensatory changes occur in the brains of older DKO mice, thus attenuating changes in expression of *Srebp-1c*, *Scd-1*, and *Egr-1*.

Loss of ABCG1 and/or ABCG4 affects brain sterol composition

The finding that the expression of genes involved in 24- or 27-hydroxylation of cholesterol (*Cyp46a* and *Cyp27a1*, respectively) or in lanosterol demethylation (*Cyp51*) were differentially expressed in the brains of DKO mice (Fig. 7) suggested that loss of these transporters will affect sterol composition. Indeed, quantification of numerous sterols using isotope dilution-mass spectrometry show that the brains from DKO mice contained increased concentrations of 24(S)-hydroxycholesterol, 25-hydroxycholesterol, 27-hydroxycholesterol, and lathosterol (**Table 2**). As expected, the changes in these sterols were greater in DKO mice compared with $Abcg1^{-/-}$ or $Abcg4^{-/-}$ mice (Table 2). Additional preliminary analyses indicate that there is an increase in 7-dehydrocholesterol and testis meiosis-activating sterol, an intermediate between lanosterol and zymosterol, as well as a decrease in campesterol in the brains of DKO mice (data not shown). We also noted that, when compared with wild-type or $Abcg1^{-/-}$ mice, total brain cholesterol levels (μg/mg wet weight) were reduced in the mice lacking ABCG4 (Table 2). This contrasts with the data of Wang et al. (15) who reported no change in cholesterol levels (μg/mg dry weight) in $Abcg4^{-/-}$ mice.

Functional changes associated with loss of ABCG1 and/or ABCG4

Changes in sterol levels and/or sterol precursors are known to affect synaptic plasticity (39). The latter is deter-
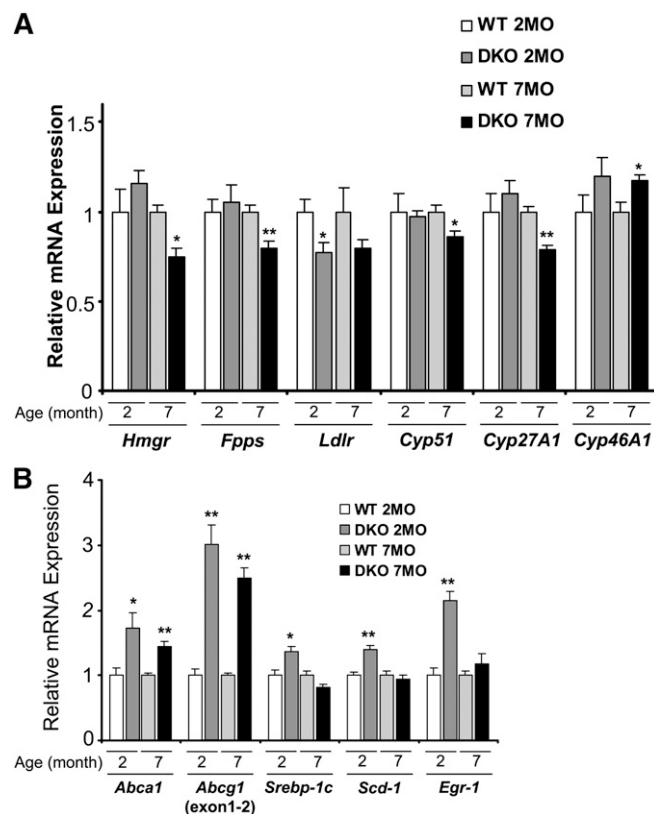
TABLE 2. Sterol levels are altered in the brains of $Abcg1^{-/-}$, $Abcg4^{-/-}$, and $Abcg1^{-/-}Abcg4^{-/-}$ mice

Sterol	Wild Type (n = 5)	$Abcg1^{-/-}$ (n = 5)	$Abcg4^{-/-}$ (n = 5)	Wild-Type (n = 9)	$Abcg1^{-/-}Abcg4^{-/-}$ (n = 9)
Cholesterol	14.5 ± 0.2	14.3 ± 1	12.7 ± 0.7*	14.4 ± 0.3	13.5 ± 0.2*
24(S)-OH-cholesterol	33.5 ± 1.2	34.7 ± 1	31.7 ± 1.4	41.3 ± 1.6	47 ± 1*
25-OH-cholesterol	0.04 ± 0.01	0.05 ± 0.02	0.03 ± 0.004	0.01 ± 0	0.02 ± 0.01*
27-OH-cholesterol	0.3 ± 0.01	0.5 ± 0.01****	0.3 ± 0.01	0.33 ± 0.01	0.42 ± 0.01****
Lathosterol				18.74 ± 0.8	24.81 ± 1.3***

Half brains were removed from 8 month old wild-type, $Abcg1^{-/-}$, and $Abcg4^{-/-}$ mice (n = 5/group). Half brains were also obtained from 8 month old $Abcg1^{-/-}Abcg4^{-/-}$ and wild-type mice (n = 9/group). Sterols were extracted and analyzed using isotope dilution-mass spectrometry (24–26). Data are presented as µg (cholesterol) or ng (other sterols) per mg of wet weight tissue. Values shown are mean ± SEM. *$P < 0.05$; **$P < 0.005$;***$P < 0.001$;****$P < 0.0005$.

mined using long-term potentiation (LTP) or long-term depression to assess synaptic strengthening or synaptic weakening, respectively. Indeed, loss of cholesterol 24-hydroxylase has a dramatic effect on LTP that can be reversed in vitro by administration of the polyisoprenoid geranylgeraniol (40). However, despite the finding that loss of both ABCG1 and ABCG4 leads to changes in brain sterol composition, there was no difference in LTP when the studies were performed using hippocampal slices from 8 month old wild-type and DKO mice (data not shown).

To assess whether loss of ABCG1 and/or ABCG4 affected other functions, we performed behavioral phenotyping on wild-type, single, and DKO 7 month old mice. Learning and memory were assessed through a Pavlovian fear conditioning procedure. This multiphase assay has been widely used to assess simple learning, such as contextual fear conditioning, a process that has been linked to hippocampal-dependent neuronal activity (41–43). In addition, Morris water maze tests were performed using 14 wild-type and 14 DKO mice. No significant differences were noted between these two genotypes in the latter test (data not shown).

Conditional fear phenotyping

Learning and memory were assessed through a Pavlovian fear conditioning procedure, a multiphase assay that characterizes various processes, including elemental and contextual associative learning, short-term memory, and memory extinction. General activity patterns were assessed prior to conditioning. All knockout and wild-type mice displayed comparable velocity ($P > 0.8$) and path shape profiles ($P > 0.5$; **Fig. 8A**) across the 3 min baseline period, when placed in a new environment (chamber), suggesting normal motor function. Similarly, all groups displayed equivalent preference for the periphery of the chamber ($P > 0.5$; data not shown), indicating comparable spatial processing in wild-type and single or DKO mice. Subsequent fear conditioning (three tone and foot shock pairings) produced robust shifts in activity. Analysis of the postshock period revealed lower levels of immobility in $Abcg4^{-/-}$ compared with the $Abcg1^{-/-}$ ($P < 0.01$) and wild-type mice ($P < 0.07$; Fig. 8B, left panel). As shown in Fig. 8B (right panel), $Abcg4^{-/-}$ mice exhibited a significant difference in turn angle relative to both wild-type and $Abcg1^{-/-}$ mice ($P < 0.01$) when tested at the same time. On the four consecutive days following training (days 2–5 in Fig. 8C), mice were returned to the conditioning chamber for 6 min to assess context fear. $Abcg4^{-/-}$ mice displayed a significant

decrease in freezing (increased mobility) compared with other genotypes, on day 2 (Fig. 8C, left panel) consistent with a persistent memory deficit ($P < 0.01$). This memory deficit, observed between $Abcg4^{-/-}$ and wild-type or DKO mice, persisted from day 2 through day 4 (Fig. 8C, right panel). By the final test session (day 5), $Abcg4^{-/-}$ mice did not differ significantly from the wild type ($P > 0.3$; Fig. 8C, right panel).

Context generalization was assessed in separate subsequent experiments by exposing mice to a novel chamber prior to cued fear testing (exposure to tone only). In contrast to the observed context fear deficits, $Abcg4^{-/-}$ mice again displayed significantly reduced immobility relative to DKO mice ($P < 0.05$), yet were nearly identical to the wild type ($P > 0.9$; Fig. 8D, left panel). Interestingly, the level of immobility of $Abcg1^{-/-}$ mice was much higher than that of the $Abcg4^{-/-}$ mice, although the difference did not reach statistical significance (Fig. 8D, left panel). Subsequent cued fear testing produced high levels of immobility across the six tone presentations (Fig. 8D); however, the levels of immobility did not differ across all four genotypes (Fig. 8D, right panel). Path shape analysis revealed comparable profiles in all groups ($P > 0.7$; data not shown). Together, these studies identify a defect in associative fear memory in $Abcg4^{-/-}$ mice. The absence of such changes in the DKO mice is unexpected and suggests that the loss of ABCG1 partially compensates for the loss of ABCG4. Whether such compensation is a result of cellular changes in other oxysterols or lipids will require additional experimentation. However, it is clear that the different behavior is not a result of gross differential expression of ABCG1 and ABCG4 in the amygdala as both genes are expressed in a similar pattern throughout this area of the brain (see supplementary Fig. I).

DISCUSSION

Previous studies have shown that in adult mice, ABCG4 expression is limited to astrocytes and neurons of the CNS (17, 18). Although ABCG1 is highly expressed in these same cells in adult mice, ABCG1 is also expressed in many other tissues and cell types, including macrophages, Type II, endothelial, and epithelial cells (13, 14, 21). In an attempt to better understand the relationship between ABCG1 and ABCG4, we investigated the expression of both genes during mouse development using mice in which the endogenous genes were disrupted following insertion of the bacterial gene encoding β-galactosidase.
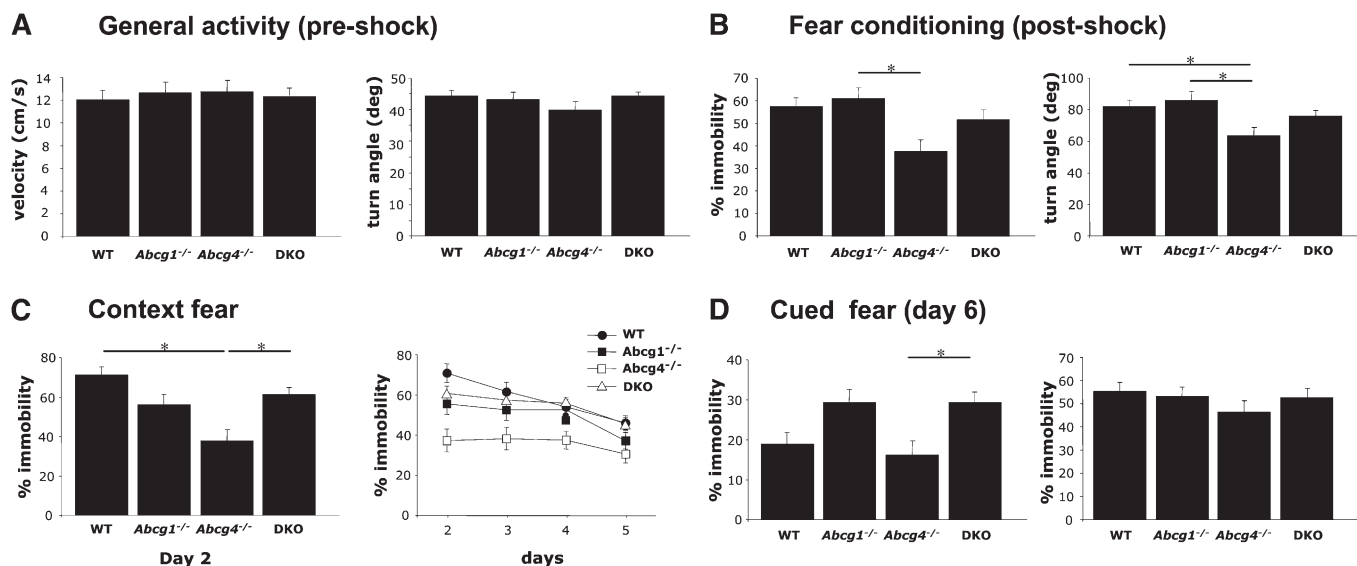
Fig. 8. Contextual fear is altered in $Abcg4^{-/-}$ mice. Wild-type (n = 10), $Abcg1^{-/-}$ (n = 7), $Abcg4^{-/-}$ (n = 6), and $Abcg1^{-/-} Abcg4^{-/-}$ (DKO) (n = 14) 7 month old mice were analyzed in a battery of behavioral tests, as described in Experimental Procedures. A: General activity as indexed by mean velocity (left) and mean turn angle (right) across the 3 min preshock period. Error bars represent SEM. B: Fear conditioning; was assessed by measuring immobility (left) and turn angle (right) across the three tone-shock pairings. C: Context fear and extinction; immobility during a 6 min reexposure to the training context 24 h after conditioning (left) and during three additional context reexposures at 24 h intervals (right). D: Context generalization and cued fear. Immobility during a 3 min exposure to a novel context (left). Immobility across the six tone presentations (Right). Values are given as mean ± SEM. * $P < 0.05$.

This approach identified cells outside the CNS, namely, hematopoietic cells in the fetal liver and enterocytes in the fetal intestine, that express ABCG4 in the absence of detectable ABCG1 (Figs. 1 and 2). These results suggest that ABCG1 and ABCG4 play distinct roles during development. The data also suggest that expression of ABCG4 outside the CNS reflects a specific temporal requirement for this transporter. Nonetheless, the physiological importance of this differential expression of ABCG1 and ABCG4 remains to be determined.

In this study, we used both in situ hybridization and assays for β-galactosidase activity to demonstrate that ABCG1 and ABCG4 are both highly expressed in the developing and adult neural retina (Fig. 4). Moreover, both transporters share the same pattern of expression, suggesting that they may form heterodimers and/or homodimers that have overlapping roles in this tissue. Surprisingly, the disruption of both ABCG1 and ABCG4 has no effect on the retinal structure or function, as determined by electron microscopy and ERG, respectively (Fig. 5). These data contrast with the changes in structure and function of the retina that follows from disruption of ABCA4 (ABCR) in albino, but not C57BL/6, mice (37). ABCA4 normally transports an *N*-retinylidene-phosphatidylethanolamine complex across the disk membranes (36, 37). Despite the lack of functional changes, we do show that loss of both ABCG1 and ABCG4 from the retina results in the accumulation of a cholesterol precursor, lathosterol, in altered expression of a stress-induced gene and in increased expression of specific LXR target genes (Table 1, Fig. 6). Together, these data suggest that the retinas of these mice accumulate oxysterols that serve as ligands for the nuclear receptor LXR. This proposal is consistent with previous

studies that have linked the accumulation of oxysterols in macrophages isolated from $Abcg1^{-/-}$ or $Abcg1^{-/-} Abca1^{-/-}$ mice to increased apoptosis (19, 44, 45). Our inability to measure changes in oxysterol levels in the retinas of $Abcg1^{-/-} Abcg4^{-/-}$ mice may simply demonstrate that very small changes in oxysterol levels within a subcellar compartment can have significant effects on gene expression.

Consistent with this latter proposal, we show that the brains of $Abcg1^{-/-} Abcg4^{-/-}$ mice accumulate not only lathosterol, but also 24-hydroxycholesterol, 25-hydroxycholesterol, and 27-hydroxycholesterol (Table 2) and 7-dehydrocholesterol, desmosterol, and testis meiosis-activating sterol (data not shown). These results extend a recent report by Wang et al. (15), which showed that the brains of 4 month old $Abcg1^{-/-} Abcg4^{-/-}$ mice accumulate desmosterol, lathosterol, and 27-hydroxycholesterol. These same authors also showed that primary cultured astrocytes isolated from the DKO mice were deficient in effluxing desmosterol and cholesterol to HDL, exhibited reduced cholesterol biosynthesis, but increased expression of ABCA1 and ABCG1 and secretion of apolipoprotein E (15).

Side-chain oxidized oxysterols are known to pass lipophilic membranes at rates orders of magnitude faster than cholesterol itself (46, 47), and the need for an active transport over cell membranes thus appears to be less important for oxysterols than for cholesterol. The result of the present work as well as that of the work by Wang et al. (15) support the contention that efflux of oxysterols may be facilitated by ABCG1 and ABCG4. Thus, there was a significant accumulation of the three side chain oxidized oxysterols 24(*S*)-, 25-, and 27-hydroxycholesterol in the brains of the $Abcg1^{-/-} Abcg4^{-/-}$ mice. There was also an increase

in 24(*S*)-hydroxycholesterol in the retina of these mice, although the change did not quite reach statistical significance.

The accumulation of multiple oxysterols and desmosterol in the brains of the DKO mice (Table 2) (15) likely accounts for the observed increased expression of selective LXR target genes that include *Abca1* and *Srebp-1c*. The finding that numerous genes in the cholesterol biosynthetic pathway are repressed in the brains of 7 month old DKO mice is consistent with a decrease in expression of mature SREBP-2, a transcription factor known to regulate these same genes (48). These changes in cholesterogenic genes is age dependent as the mRNA levels of 2 month old DKO and wild-type mice are not significantly different (Table 2). Indeed, these age-dependent changes in the brain are reminiscent of the age-dependent accumulation of cholesterol, phospholipids, and inflammatory genes that have been shown to occur in the lungs of $Abcg1^{-/-}$ mice (44, 49). The finding that aberrant expression of genes involved in cholesterol synthesis and uptake is more pronounced in the brains compared with the retinas of DKO mice suggests that cholesterol homeostasis in the brain is more dependent than the retina upon these two ABC transporters. Consistent with this proposal, cholesterol in the brain is known to be derived from de novo synthesis within the organ, since the brain is isolated from the systemic circulation by the blood-brain barrier that prevents passage of cholesterol from plasma lipoproteins into the brain (1). In contrast, cells in the retina can obtain cholesterol from both systemic circulation and de novo synthesis; however, the relative contribution of these two pathways to sterol homeostasis in the retina is not known (6). In addition, as a result of the blood-brain barrier, efflux of sterols from the brain to the blood may be impaired compared with sterol efflux from the retina. Such a difference might account for the more pronounced changes in sterol levels and altered expression of specific mRNAs (e.g., *Ldlr*) in the brain compared with the retina (Figs. 6 and 7).

The adverse effects that result from loss of functional ABCG1 and ABCG4 from the CNS might well be ameliorated in part by the increased expression of ABCA1 that would be expected to increase the efflux of sterols and phospholipids from astrocytes and neurons to apolipoprotein E-rich lipoproteins in the cerebrospinal fluid. However, it appears that increased expression of ABCA1 in the lung (15) or brain (Fig. 7) in response to deletion of ABCG4 and/or ABCG1 cannot adequately maintain cellular sterol levels. Whether this is because the ABCG1, ABCG4, and ABCA1 transport different sterols (15, 50) or whether it is simply a defect in the overall ability to efflux sterol mass remains unclear. Nonetheless, the data indicate that cells of the brain utilize numerous sterol-transport pathways, including those regulated by ABCG1, ABCG4, and ABCA1, to maintain critical intracellular sterol levels.

Cholesterol has long been thought to play a critical function in the CNS (39). Thus, the generation of viable mice that contain <3% of normal cholesterol as a result of deletion of desmosterol reductase, *Dhcr24*, the last enzyme in the cholesterol biosynthetic pathway, was remarkable (51). Nonetheless, various natural mutations in genes affecting sterol homeostasis in humans and/or gene knockouts in mice indicate that altered sterol homeostasis in the CNS often affects neuronal function (3). Surprisingly, results from this study identify only one physiological effect resulting from disruption of both *Abcg1* and *Abcg4* genes in mice. The data demonstrate a specific memory defect in $Abcg4^{-/-}$ mice. The pronounced contextual fear deficits suggest that ABCG4 contributes significantly to processes mediating the acquisition and/or expression of contextual fear. The observed immobility deficits do not appear to stem from reduced pain sensitivity, as the $Abcg4^{-/-}$ mice exhibited normal shock-induced activity bursts ($P > 0.8$). Nor are they the product of a general deficit in production of the fear response, as $Abcg4^{-/-}$ mice exhibited normal immobility levels during tone presentations. Hyperactivity does not account for the deficit given the normal velocity and path shape profiles. Likewise, a general defect in the processing of contextual information is not a likely source of the deficit considering the normal place preference levels observed prior to conditioning. Rather, the phenotype exhibited by $Abcg4^{-/-}$ mice suggests an effect for this gene on processes related to neuronal plasticity underlying long-term contextual memory storage.

The original observations that overexpression of ABCG1 or ABCG4 in cultured cells promotes the efflux of cellular cholesterol to HDL led to the proposal that ABCG1 might be involved in efflux of cellular cholesterol to HDL and possibly other plasma lipoproteins (24). However, numerous studies have now shown that plasma lipoprotein levels are unaltered in transgenic mice that overexpress ABCG1 from a human BAC or lack ABCG1 and/or ABCG4 as a result of disruption of the endogenous genes (49, 52, 53). Thus, the current evidence suggests that ABCG1 and ABCG4 function primarily to control intracellular sterol movement and homeostasis and play little, if any, role in regulating plasma lipoprotein levels. The current studies are consistent with this proposal and indicate that both ABCG4 and ABCG1 are important for neuronal cell function.

REFERENCES

1. Dietschy, J. M., and S. D. Turley. 2001. Cholesterol metabolism in the brain. *Curr. Opin. Lipidol.* **12:** 105–112.
2. Bjorkhem, I., and E. Leitersdorf. 2000. Sterol 27-hydroxylase deficiency: a rare cause of xanthomas in normocholesterolemic humans. *Trends Endocrinol. Metab.* **11:** 180–183.
3. Porter, F. D. 2003. Human malformation syndromes due to inborn errors of cholesterol synthesis. *Curr. Opin. Pediatr.* **15:** 607–613.
4. Krakowiak, P. A., C. A. Wassif, L. Kratz, D. Cozma, M. Kovarova, G. Harris, A. Grinberg, Y. Yang, A. G. Hunter, M. Tsokos, et al. 2003. Lathosterolosis: an inborn error of human and murine cholesterol synthesis due to lathosterol 5-desaturase deficiency. *Hum. Mol. Genet.* **12:** 1631–1641.

5. Lund, E. G., C. Xie, T. Kotti, S. D. Turley, J. M. Dietschy, and D. W. Russell. 2003. Knockout of the cholesterol 24-hydroxylase gene in mice reveals a brain-specific mechanism of cholesterol turnover. *J. Biol. Chem.* **278:** 22980–22988.

6. Fliesler, S. J., and R. K. Keller. 1997. Isoprenoid metabolism in the vertebrate retina. *Int. J. Biochem. Cell Biol.* **29:** 877–894.

7. Albert, A. D., and K. Boesze-Battaglia. 2005. The role of cholesterol in rod outer segment membranes. *Prog. Lipid Res.* **44:** 99–124.

8. Giusto, N. M., S. J. Pasquare, G. A. Salvador, P. I. Castagnet, M. E. Roque, and M. G. Ilincheta de Boschero. 2000. Lipid metabolism in vertebrate retinal rod outer segments. *Prog. Lipid Res.* **39:** 315–391.

9. Dean, M., and R. Allikmets. 2001. Complete characterization of the human ABC gene family. *J. Bioenerg. Biomembr.* **33:** 475–479.

10. Cserepes, J., Z. Szentpetery, L. Seres, C. Ozvegy-Laczka, T. Langmann, G. Schmitz, H. Glavinas, I. Klein, L. Homolya, A. Varadi, et al. 2004. Functional expression and characterization of the human ABCG1 and ABCG4 proteins: indications for heterodimerization. *Biochem. Biophys. Res. Commun.* **320:** 860–867.

11. Ewart, G. D., and A. J. Howells. 1998. ABC transporters involved in transport of eye pigment precursors in Drosophila melanogaster. *Methods Enzymol.* **292:** 213–224.

12. Tarr, P. T., E. J. Tarling, D. D. Bojanic, P. A. Edwards, and A. Baldan. 2009. Emerging new paradigms for ABCG transporters. *Biochem. Biophys. Acta* **1791:** 584–593.

13. Kennedy, M. A., G. C. Barrera, K. Nakamura, A. Baldan, P. Tarr, M. C. Fishbein, J. Frank, O. L. Francone, and P. A. Edwards. 2005. ABCG1 has a critical role in mediating cholesterol efflux to HDL and preventing cellular lipid accumulation. *Cell Metab.* **1:** 121–131.

14. Nakamura, K., M. A. Kennedy, A. Baldan, D. D. Bojanic, K. Lyons, and P. A. Edwards. 2004. Expression and regulation of multiple murine ATP-binding cassette transporter G1 mRNAs/isoforms that stimulate cellular cholesterol efflux to high density lipoprotein. *J. Biol. Chem.* **279:** 45980–45989.

15. Wang, N., L. Yvan-Charvet, D. Lutjohann, M. Mulder, T. Vanmierlo, T. W. Kim, and A. R. Tall. 2008. ATP-binding cassette transporters G1 and G4 mediate cholesterol and desmosterol efflux to HDL and regulate sterol accumulation in the brain. *FASEB J.* **22:** 1073–1082.

16. Annilo, T., J. Tammur, A. Hutchinson, A. Rzhetsky, M. Dean, and R. Allikmets. 2001. Human and mouse orthologs of a new ATP-binding cassette gene, ABCG4. *Cytogenet. Cell Genet.* **94:** 196–201.

17. Oldfield, S., C. Lowry, J. Ruddick, and S. Lightman. 2002. ABCG4: a novel human white family ABC-transporter expressed in the brain and eye. *Biochim. Biophys. Acta.* **1591:** 175–179.

18. Tarr, P. T., and P. A. Edwards. 2008. ABCG1 and ABCG4 are coexpressed in neurons and astrocytes of the CNS and regulate cholesterol homeostasis through SREBP-2. *J. Lipid Res.* **49:** 169–182.

19. Baldan, A., P. Tarr, C. S. Vales, J. Frank, T. K. Shimotake, S. Hawgood, and P. A. Edwards. 2006. Deletion of the transmembrane transporter ABCG1 results in progressive pulmonary lipidosis. *J. Biol. Chem.* **281:** 29401–29410.

20. Out, R., M. Hoekstra, I. Meurs, P. de Vos, J. Kuiper, M. Van Eck, and T. J. Van Berkel. 2007. Total body ABCG1 expression protects against early atherosclerotic lesion development in mice. *Arterioscler. Thromb. Vasc. Biol.* **27:** 594–599.

21. Gelissen, I. C., M. Harris, K. A. Rye, C. Quinn, A. J. Brown, M. Kockx, S. Cartland, M. Packianathan, L. Kritharides, and W. Jessup. 2006. ABCA1 and ABCG1 synergize to mediate cholesterol export to apoA-I. *Arterioscler. Thromb. Vasc. Biol.* **26:** 534–540.

22. Vaughan, A. M., and J. F. Oram. 2005. ABCG1 redistributes cell cholesterol to domains removable by high density lipoprotein but not by lipid-depleted apolipoproteins. *J. Biol. Chem.* **280:** 30150–30157.

23. Vaughan, A. M., and J. F. Oram. 2006. ABCA1 and ABCG1 or ABCG4 act sequentially to remove cellular cholesterol and generate cholesterol-rich HDL. *J. Lipid Res.* **47:** 2433–2443.

24. Wang, N., D. Lan, W. Chen, F. Matsuura, and A. R. Tall. 2004. ATP-binding cassette transporters G1 and G4 mediate cellular cholesterol efflux to high-density lipoproteins. *Proc. Natl. Acad. Sci. USA.* **101:** 9774–9779.

25. Uehara, Y., T. Yamada, Y. Baba, S. Miura, S. Abe, K. Kitajima, M. A. Higuchi, T. Iwamoto, and K. Saku. 2008. ATP-binding cassette transporter G4 is highly expressed in microglia in Alzheimer's brain. *Brain Res.* **1217:** 239–246.

26. Schaffer, R., L. T. Sniegoski, M. J. Welch, V. E. White, A. Cohen, H. S. Hertz, J. Mandel, R. C. Paule, L. Svensson, I. Bjorkhem, et al. 1982. Comparison of two isotope dilution/mass spectrometric methods for determination of total serum cholesterol. *Clin. Chem.* **28:** 5–8.

27. Lund, E., L. Sisfontes, E. Reihner, and I. Bjorkhem. 1989. Determination of serum levels of unesterified lathosterol by isotope dilution-mass spectrometry. *Scand. J. Clin. Lab. Invest.* **49:** 165–171.

28. Dzeletovic, S., O. Breuer, E. Lund, and U. Diczfalusy. 1995. Determination of cholesterol oxidation products in human plasma by isotope dilution-mass spectrometry. *Anal. Biochem.* **225:** 73–80.

29. Kedzierski, W., M. Lloyd, D. G. Birch, D. Bok, and G. H. Travis. 1997. Generation and analysis of transgenic mice expressing P216L-substituted rds/peripherin in rod photoreceptors. *Invest. Ophthalmol. Vis. Sci.* **38:** 498–509.

30. Nusinowitz, S., W. H. Ridder 3rd, and J. Ramirez. 2007. Temporal response properties of the primary and secondary rod-signaling pathways in normal and Gnat2 mutant mice. *Exp. Eye Res.* **84:** 1104–1114.

31. Anagnostaras, S. G., S. A. Josselyn, P. W. Frankland, and A. J. Silva. 2000. Computer-assisted behavioral assessment of Pavlovian fear conditioning in mice. *Learn. Mem.* **7:** 58–72.

32. Nie, T., and T. Abel. 2001. Fear conditioning in inbred mouse strains: an analysis of the time course of memory. *Behav. Neurosci.* **115:** 951–956.

33. Choi, S. H., M. T. Woodlee, J. J. Hong, and T. Schallert. 2006. A simple modification of the water maze test to enhance daily detection of spatial memory in rats and mice. *J. Neurosci. Methods.* **156:** 182–193.

34. Annicotte, J. S., K. Schoonjans, and J. Auwerx. 2004. Expression of the liver X receptor alpha and beta in embryonic and adult mice. *Anat. Rec. A Discov. Mol. Cell. Evol. Biol.* **277:** 312–316.

35. Westerfeld, C., and S. Mukai. 2008. Stargardt's disease and the ABCR gene. *Semin. Ophthalmol.* **23:** 59–65.

36. Weng, J., N. L. Mata, S. M. Azarian, R. T. Tzekov, D. G. Birch, and G. H. Travis. 1999. Insights into the function of Rim protein in photoreceptors and etiology of Stargardt's disease from the phenotype in abcr knockout mice. *Cell.* **98:** 13–23.

37. Radu, R. A., Q. Yuan, J. Hu, J. H. Peng, M. Lloyd, S. Nusinowitz, D. Bok, and G. H. Travis. 2008. Accelerated accumulation of lipofuscin pigments in the RPE of a mouse model for ABCA4-mediated retinal dystrophies following Vitamin A supplementation. *Invest. Ophthalmol. Vis. Sci.* **49:** 3821–3829.

38. Tontonoz, P., and D. J. Mangelsdorf. 2003. Liver X receptor signaling pathways in cardiovascular disease. *Mol. Endocrinol.* **17:** 985–993.

39. Pfrieger, F. W. 2003. Role of cholesterol in synapse formation and function. *Biochim. Biophys. Acta.* **1610:** 271–280.

40. Kotti, T. J., D. M. Ramirez, B. E. Pfeiffer, K. M. Huber, and D. W. Russell. 2006. Brain cholesterol turnover required for geranylgeraniol production and learning in mice. *Proc. Natl. Acad. Sci. USA.* **103:** 3869–3874.

41. Anagnostaras, S. G., G. D. Gale, and M. S. Fanselow. 2001. Hippocampus and contextual fear conditioning: recent controversies and advances. *Hippocampus.* **11:** 8–17.

42. Marschner, A., R. Kalisch, B. Vervliet, D. Vansteenwegen, and C. Buchel. 2008. Dissociable roles for the hippocampus and the amygdala in human cued versus context fear conditioning. *J. Neurosci.* **28:** 9030–9036.

43. O'Reilly, R. C., and J. W. Rudy. 2001. Conjunctive representations in learning and memory: principles of cortical and hippocampal function. *Psychol. Rev.* **108:** 311–345.

44. Wojcik, A. J., M. D. Skaflen, S. Srinivasan, and C. C. Hedrick. 2008. A critical role for ABCG1 in macrophage inflammation and lung homeostasis. *J. Immunol.* **180:** 4273–4282.

45. Yvan-Charvet, L., M. Ranalletta, N. Wang, S. Han, N. Terasaka, R. Li, C. Welch, and A. R. Tall. 2007. Combined deficiency of ABCA1 and ABCG1 promotes foam cell accumulation and accelerates atherosclerosis in mice. *J. Clin. Invest.* **117:** 3900–3908.

46. Lange, Y., J. Ye, and F. Strebel. 1995. Movement of 25-hydroxycholesterol from the plasma membrane to the rough endoplasmic reticulum in cultured hepatoma cells. *J. Lipid Res.* **36:** 1092–1097.

47. Meaney, S., K. Bodin, U. Diczfalusy, and I. Bjorkhem. 2002. On the rate of translocation in vitro and kinetics in vivo of the major oxysterols in human circulation: critical importance of the position of the oxygen function. *J. Lipid Res.* **43:** 2130–2135.

48. Horton, J. D., J. L. Goldstein, and M. S. Brown. 2002. SREBPs: activators of the complete program of cholesterol and fatty acid synthesis in the liver. *J. Clin. Invest.* **109:** 1125–1131.

49. Baldan, A., D. D. Bojanic, and P. A. Edwards. 2008. The ABCs of sterol transport. *J. Lipid Res.* **50** (Suppl.): S80–S85.
50. Engel, T., F. Kannenberg, M. Fobker, J. R. Nofer, G. Bode, A. Lueken, G. Assmann, and U. Seedorf. 2007. Expression of ATP binding cassette-transporter ABCG1 prevents cell death by transporting cytotoxic 7beta-hydroxycholesterol. *FEBS Lett.* **581:** 1673–1680.
51. Heverin, M., S. Meaney, A. Brafman, M. Shafir, M. Olin, M. Shafaati, S. von Bahr, L. Larsson, A. Lovgren-Sandblom, U. Diczfalusy, et al. 2007. Studies on the cholesterol-free mouse: strong activation of LXR-regulated hepatic genes when replacing cholesterol with desmosterol. *Arterioscler. Thromb. Vasc. Biol.* **27:** 2191–2197.
52. Basso, F., M. J. Amar, E. M. Wagner, B. Vaisman, B. Paigen, S. Santamarina-Fojo, and A. T. Remaley. 2006. Enhanced ABCG1 expression increases atherosclerosis in LDLr- KO mice on a western diet. *Biochem. Biophys. Res. Commun.* **351:** 398–404.
53. Burgess, B., K. Naus, J. Chan, V. Hirsch-Reinshagen, G. Tansley, L. Matzke, B. Chan, A. Wilkinson, J. Fan, J. Donkin, et al. 2008. Overexpression of human ABCG1 does not affect atherosclerosis in fat-fed ApoE-deficient mice. *Arterioscler. Thromb. Vasc. Biol.* **28:** 1731–1737.